Analysis of a static undulation on the surface of a thin dielectric liquid layer formed by dielectrophoresis forces

Carl V. Brown[*,#], Glen McHale[*] and Nigel J. Mottram[$]

[*]*School of Science and Technology, Nottingham Trent University, Erasmus Darwin Building, Clifton Lane, Clifton, Nottingham, NG11 8NS, UK*

[$]*Department of Mathematics and Statistics, University of Strathclyde, Livingstone Tower, 26 Richmond Street, Glasgow G1 1XH, UK*

Abstract

A layer of insulating liquid of dielectric constant ε_{Oil} and average thickness $\bar{h}$ coats a flat surface at y = 0 at which a 1-dimensional sinusoidal potential $V(x,0)=V_O\cos(\pi x/p)$ is applied. Dielectrophoresis forces create a static undulation (or "wrinkle") distortion $h(x)$ of period p at the liquid/air interface. Analytical expressions have been derived for the electrostatic energy and the interfacial energy associated with the surface undulation when $h(x)=\bar{h}-\frac{1}{2}A\cos(2\pi x/p)$ yielding a scaling relationship for A as a function of $\bar{h}$, p, V_O, ε_{Oil} and the surface tension. The analysis is valid as $A/p \to 0$, and in this limit convergence with numerical simulation of the system is shown.

[#] Telephone: 44 (0)115 8483184 E-mail: carl.brown@ntu.ac.uk

Keywords: *Liquid dielectrophoresis, electrostatic energy, surface tension, liquid thin films*

1. Introduction

The action of dielectrophoresis forces on insulating liquids has been used to move and distort liquid droplets, for example to draw a "finger" of liquid between co-planar electrodes [1] [2], or to cause the droplet to wet a solid surface on which there is a patterned interdigital array of co-planar electrodes in order to produce liquid optical devices [3] [4] [5] [6]. Dielectrophoresis forces arise in dielectric materials that are polarised in regions in which there are gradients in the electric field [7] [8]. Such highly non-uniform "fringing" electric fields are created predominantly in the regions between the coplanar electrodes in these geometries.

We have previously shown that an interdigital array of striped co-planar electrodes can be used to spread a droplet of oil into a thin uniform film and that a static periodic deformation, or wrinkle, forms on the spread film at the oil/air interface [5]. The period p of the wrinkle was found to be equal to the period of the electrode stripes, which is half of the electrical period since neighbouring stripes on the array were oppositely biased at potentials $+V_O$ and $-V_O$. The peak to peak amplitude A of the wrinkle deformation was found to depend strongly on the magnitude of the potential $|V_O|$, the average film thickness $\bar{h}$, and the pitch p [9].

In the current paper a theoretical model of the system is developed using the key simplifications that the potential on the lower boundary of the film of the dielectric liquid and the wrinkle deformation at the liquid/air interface are both a sinusoidal function of the spatial coordinate x. This model enables analytical expressions to be derived that elucidate the dependence of the energy and the amplitude A on the key geometric and materials parameters.

2. Numerical simulation

The model geometry that has been investigated is shown in figure 1. This is a 2-dimensional geometry in the x-y plane which is assumed to be infinite in the z-direction. A layer of insulating dielectric liquid of average thickness $\bar{h}$ coats the flat solid surface at $y = 0$. The air space above the liquid continues to infinity in the positive y-direction. A sinusoidal potential $V(x,0) = -V_O \cos(½kx)$ is applied at the lower boundary of the liquid, $y = 0$, where $k = 2\pi/p$. A sinusoidal distortion with peak to peak amplitude A is imposed at the liquid/air interface giving an oil film thickness $h(x)$ as described by equation [1].

$$h(x) = \bar{h} - ½A\cos(kx) \qquad [1]$$

The choice of the phase of distortion described by equation [1] relative to the potential has been pre-determined from the numerical simulations. The height of the liquid $h(x)$ is increased above the positions where there are the highest gradients in the potential at $x = \pm ½np$ where n is an integer. Liquid collects in these regions and is removed from the regions around $x = \pm np$ where there is a reduction in $h(x)$.

The potential $V(x, y)$ has been calculated from an iterative numerical solution of the discretised form of the Maxwell equation [2] in the half space $y > 0$ using standard methods [10].

$$\nabla \cdot \left(-\varepsilon_o \varepsilon \nabla V(x, y)\right) = 0 \qquad [2]$$

where ε is the dielectric constant obtaining at position (x, y), i.e. $\varepsilon = \varepsilon_{oil}$ when $y < h(x)$ and $\varepsilon = \varepsilon_{air}$ when $y > h(x)$. Periodic boundary conditions are applied connecting the right and left-hand boundaries in figure 1, $(p, y) \equiv (-p, y)$. An example potential profile $V(x, y)$ is shown in figure 2 that was calculated numerically for a liquid with permittivity $\varepsilon_{oil} = 8$, with $\bar{h} / p = 0.5$, $p = 80$ μm, and with a sinusoidal liquid/air interfacial distortion for which $Ak = 0.5$. In practice the calculation must be performed in a finite region and an upper interface was placed at $y = 10p$ at which the potential was set at zero, $V(x, 10p) = 0$ V. The peak voltage was set at $V_O = 1.0$ V giving a potential of 1.0 V at (0, 0) and -1.0 V at $(p, 0) \equiv (-p, 0)$.

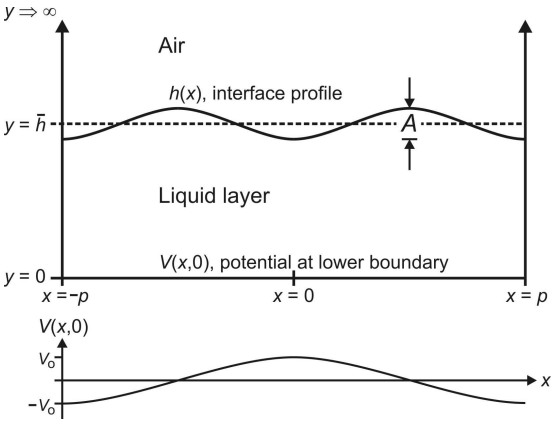

Figure 1. The model geometry. A layer of liquid of average thickness $\bar{h}$ coats a flat surface at $y = 0$. The air space continues to infinity. A sinusoidal potential $V(x,0)=V_o\cos(\pi x/p)$ is applied at $y = 0$ whilst a sinusoidal "wrinkle" distortion of period p is imposed at the liquid/air interface.

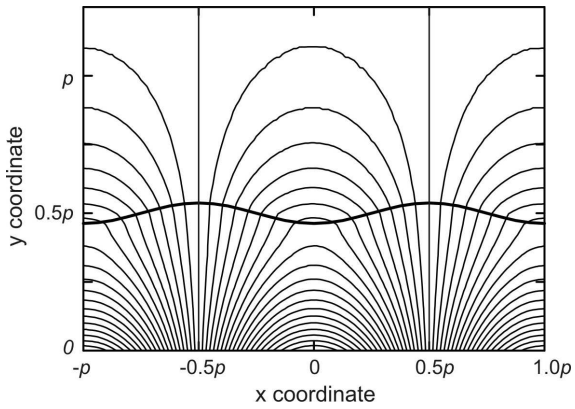

Figure 2. The potential profile $V(x, y)$ predicted by the LaPlace equation calculated for a liquid with permittivity $\varepsilon_{oil} = 8$, with $\bar{h} / p = 0.5$, $p = 80$ μm, and a sinusoidal liquid/air interfacial distortion for which $Ak = 0.5$ (where $k = 2\pi/p$). The potential was 1.0 V at (0, 0), –1.0 V at (p, 0) and ($-p$, 0) and each equipotential corresponds to a potential change of 0.05 V.

The position of the liquid/air interface $h(x)$ is shown by the thick solid line in figure 2 and the equipotentials are shown by the thin solid lines. Each equipotential indicates a potential change of 0.05 V relative to its neighbouring equipotential. The discontinuous changes in direction of the equipotentials at the liquid/air interface in figure 2 are a consequence of the electrostatic boundary conditions and the mismatch between the dielectric constants of the oil ($\varepsilon_{oil} = 8$ was used to produce the figure) and air ($\varepsilon_{air} = 1$).

In figure 3 the solid line shows a plot of the value of the potential from figure 2 at a constant y-position just below the liquid/air interface, $V(x, y = 0.4p)$, as a function of the x-coordinate. The spatial variation in the potential is adequately described by the sum of a $\cos(kx/2)$ component and a $\cos(3kx/2)$ component shown by the dot-dot-dashed line and the short-dashed line respectively in the figure. This observation suggests an analytical approach in which the potential $V(x, y)$ in the system is expressed as a series expansion containing spatially periodic terms at least to order $\cos(3kx/2)$.

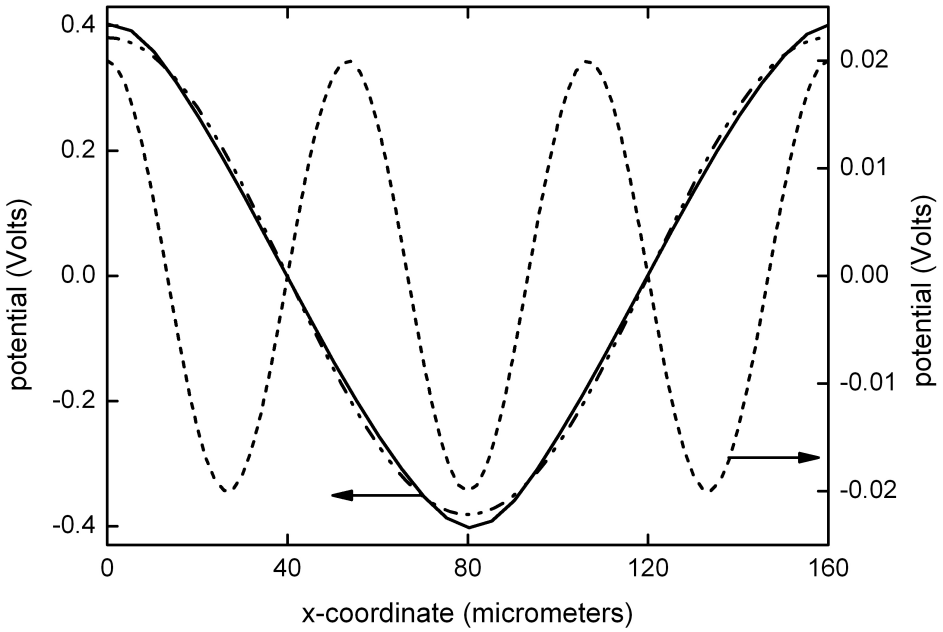

Figure 3. The solid line shows the potential at height $y = 0.4p$ as a function of the x-coordinate from figure 2. The spatial variation in the potential is adequately described by the sum of a $\cos(kx/2)$ component and a $\cos(3kx/2)$ component shown by the dot-dot-dashed line and the short-dashed line respectively (where $k = 2\pi/p$).

3. Electrostatic energy of the system

The potential in the oil layer and the potential in the air region will be described by series expansions of Fourier modes given in equations [3] and [4] respectively. The coefficients of higher order modes for which $n > 3$ are all zero to first order in Ak since the periodic potential at the lower boundary and the deformation at the oil/air interface (equation [1]) are both single mode sinusoidal functions of the coordinate x. This model system is readily accessible to analytical solution.

$$V_{\text{oil}}(x,y) = \sum_{n=1}^{3} a_n \cos(\tfrac{1}{2}nkx)\exp(-\tfrac{1}{2}nky) + \sum_{n=1}^{3} b_n \cos(\tfrac{1}{2}nkx)\exp(\tfrac{1}{2}nky) \qquad [3]$$

$$V_{\text{air}}(x,y) = \sum_{n=1}^{3} c_n \cos(\tfrac{1}{2}nkx)\exp(-\tfrac{1}{2}nky) \qquad [4]$$

where equations [3] and [4] both obey the Maxwell equation [2]. At the liquid/air interface the electrostatic boundary conditions obtain that the tangential component of the electric field and the normal component of the displacement field must both be continuous, $\mathbf{E}_{\text{oil}}(x,h(x))\cdot\hat{\mathbf{t}} = \mathbf{E}_{\text{air}}(x,h(x))\cdot\hat{\mathbf{t}}$ and $\varepsilon_{\text{oil}}\mathbf{E}_{\text{oil}}(x,h(x))\cdot\hat{\mathbf{n}} = \varepsilon_{\text{air}}\mathbf{E}_{\text{air}}(x,h(x))\cdot\hat{\mathbf{n}}$ respectively, where $\mathbf{E}_{\text{oil}}(x,h(x)) = -\nabla V_{\text{oil}}(x,h(x))$ and $\mathbf{E}_{\text{air}}(x,h(x)) = -\nabla V_{\text{air}}(x,h(x))$ are the electric fields an infinitesimal distance below and above the liquid/air interface respectively. The unit normal vector to the surface and the unit tangent vector at the surface are defined by $\hat{\mathbf{n}} = \nabla S/|\nabla S|$ and $\hat{\mathbf{t}} = \hat{\mathbf{z}}\times\hat{\mathbf{n}}$ respectively with $\hat{\mathbf{z}} = (0,0,1)$ and with the distortion of the liquid/air interface $h(x)$ in equation [1] re-written so that it is in the standard form of the equation of a surface, $S(x,y) = y + \tfrac{1}{2}A\cos(2\pi x/p) - \bar{h}$.

Expressions for the coefficients in equations [3] and [4] are derived by matching the electrostatic boundary conditions at the liquid/air interface $y = h(x)$ and at $y = 0$ where the spatially periodic potential $V(x,0) = V_O\cos(\tfrac{1}{2}kx)$ is imposed. The boundary condition at the lower interface gives

$a_1 + b_1 = V_O$, $a_2 + b_2 = 0$, and $a_3 + b_3 = 0$. It will be assumed that the peak to peak amplitude of the wrinkle is small, $Ak << 1$, and so exponential terms can be replaced by the series approximation $\exp(x) \approx 1 + x$. Equating the coefficients of sine and cosine terms that have the same arguments yields nine simultaneous equations. These have been solved to find the nine coefficients of the Fourier modes a_1, a_2, a_3, b_1, b_2, b_3, c_1, c_2 and c_3. It is found that $a_2 = 0$, $b_2 = 0$ and $c_2 = 0$ due to the symmetry of the system. Expressions for the other 6 coefficients are given to first order in Ak in the appendix (all orders of Ak are retained in the subsequent analysis unless otherwise stated). The coefficients a_3, b_3 and c_3 do not contain a constant component that is independent of Ak since the 3rd Fourier mode arises as a consequence of the presence of the wrinkle deformation at the liquid/air interface.

The electrostatic energy of the system per unit length in the z-direction is given by equation [5].

$$W_E = -\frac{\varepsilon_O \varepsilon_{\text{oil}}}{2} \int_{-2\pi/k}^{2\pi/k} \int_0^{h(x)} (\mathbf{E}_{\text{oil}} \cdot \mathbf{E}_{\text{oil}}) dy dx - \frac{\varepsilon_O \varepsilon_{\text{air}}}{2} \int_{-2\pi/k}^{2\pi/k} \int_{h(x)}^{\infty} (\mathbf{E}_{\text{air}} \cdot \mathbf{E}_{\text{air}}) dy dx \qquad [5]$$

The result of performing the double integration in equation [5] to first order in Ak is given in equation [6] where $\Delta\varepsilon = (\varepsilon_{\text{oil}} - \varepsilon_{\text{air}})/(\varepsilon_{\text{oil}} + \varepsilon_{\text{air}})$. After performing the y-integrations in equation [5] the exponential terms were replaced with Taylor series expansions, using the assumption that $Ak << 1$, before the x-integrations were performed.

$$W_E = -\frac{\pi \varepsilon_O \varepsilon_{\text{oil}}}{2} V_O^2 \left[\left(\frac{1 - \Delta\varepsilon \exp(-k\bar{h})}{1 + \Delta\varepsilon \exp(-k\bar{h})} \right) + \frac{\Delta\varepsilon^2 \exp(-k\bar{h}) Ak}{2(1 + \Delta\varepsilon \exp(-k\bar{h}))^2} \right] \qquad [6]$$

In figures 4 and 5 the ratio $-W_E/(\varepsilon_O \varepsilon_{\text{Oil}} V_O^2)$ is plotted as a function of the parameter Ak (where $k = 2\pi/p$). The solid lines show values calculated from the numerical solution of the Maxwell equation [2] as described in section 2. The dashed lines show the predictions of the analytical expression in equation [6]. The contribution to the electrostatic energy of the system when $Ak = 0$ has been subtracted so that all curves start at the origin. In figure 4 curves are shown for the ratio $\bar{h}/p$ in the range $0.03 < \bar{h}/p < 0.5$ when $\varepsilon_{\text{oil}} = 8.0$. In figure 5 curves are shown for the relative permittivity of the liquid ε_{oil} in the range $1.5 < \varepsilon_{\text{oil}} < 20$ when $\bar{h}/p = 0.25$. The values of the ratio $\bar{h}/p$ (figure 4) and ε_{oil} (figure 5) are labelled on the solid line curves for the numerical solutions.

In figure 4 the deviations between the numerical results (solid lines) and the analytical expression (dashed lines) is small when $\bar{h}/p = 0.5$, it increases as $\bar{h}/p$ is decreased below this value, reaches a maximum at intermediate values, and then the deviation is small again when $\bar{h}/p = 0.03$. Consider varying $\bar{h}/p$ with a fixed value of $Ak = 0.2$. When $\bar{h}/p = 0.5$ the ratio of the wrinkle amplitude to the film thickness is small, $A/\bar{h} = 0.064$, the wrinkle is a small perturbation to the shape of the film layer, and so the analytical expression is a good approximation. As the value of $\bar{h}/p$ and thus the layer thickness is decreased the amplitude of wrinkle distortion with a fixed value of Ak becomes more significant with respect to the layer thickness, for example $A/\bar{h} = 0.16$ when $\bar{h}/p = 0.2$. This causes greater disruption to the 2-dimensional potential profile within and above the oil layer which is rigorously calculated in the numerical solution but which leads to greater error in the analytical linear approximation.

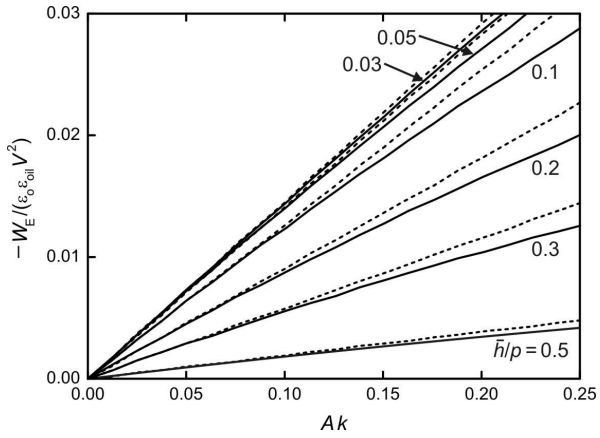

Figure 4. The scaled electrostatic energy of the system $-W_E/(\varepsilon_O\varepsilon_{Oil}V_O^2)$ as a function of the parameter Ak (where $k = 2\pi/p$). The solid lines were calculated from the numerical solution of the Maxwell equation [2] and the dashed lines show the predictions of the analytical approximation given by equation [6] for $\varepsilon_{oil} = 8.0$. The values of the ratio $\bar{h}/p$ are labelled on the numerical solutions which asymptote towards to the corresponding analytical linear solutions in the limit $A{\cdot}k \to 0$.

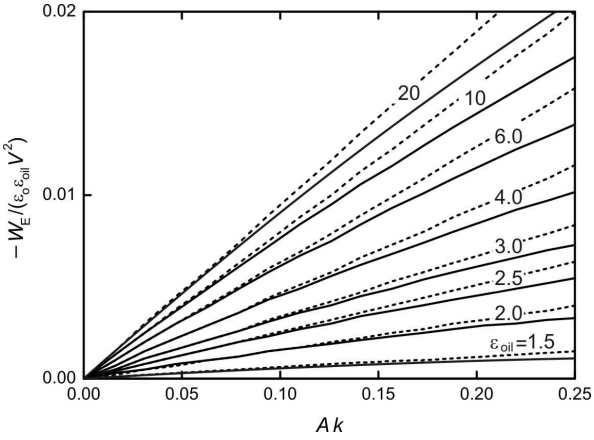

Figure 5. The scaled electrostatic energy of the system $-W_E/(\varepsilon_O\varepsilon_{Oil}V_O^2)$ as a function of the parameter Ak (where $k = 2\pi/p$). The solid lines were calculated from the numerical solution of the Maxwell equation [2] and the dashed lines show the predictions of the analytical approximation given by equation [6] for $\bar{h}/p = 0.25$. The values of the relative permittivity of liquid ε_{oil} are labelled on the numerical solutions which asymptote towards to the corresponding analytical linear solutions in the limit $Ak \to 0$.

When the ratio $\bar{h}/p$ is decreased still further this corresponds to a significant thinning of the oil layer. For example, if $Ak = 0.2$ and $\bar{h}/p = 0.03$ this gives $A = 3.2\,\mu$m and $\bar{h} = 3.0\,\mu$m when $p = 100\,\mu$m. Although the relative amplitude of the wrinkle is large there is less opportunity to distort the 2-dimension potential profile within the oil layer due to the close proximity of the oil/air interface to the lower boundary at which the potential is fixed as $V(x,0) = V_O\cos(½kx)$. Note that the condition $A/\bar{h} = (Ak)/(2\pi(\bar{h}/p)) = 2$ corresponds to "punch-through" where the wrinkle amplitude relative to the layer thickness is sufficient for the trough in the wrinkle to touch the substrate surface at $y = 0$.

The value of W_E shows a minimum for $\varepsilon_{oil} = 1.5$ in figure (5). This occurs for all the numerical solutions if the range of Ak is extended, and the numerical solutions have a parabolic dependence on Ak to a good approximation. Intuitively a minimum in the electrostatic energy would be expected at the value of A when the normal to the surface $\hat{\mathbf{n}}$ is substantially parallel to the equipotential lines. The numerical solutions shown by the solid lines asymptote towards to the corresponding analytical linear solutions shown by the dashed lines in the limit $Ak \to 0$, as expected. In this limit the gradients of the curves increase monotonically as either the ratio $\bar{h}/p$ is decreased or the value of relative permittivity of the liquid ε_{oil} is increased.

4. Geometrical and material parameter dependence of the wrinkle amplitude *A*

The length L of the oil-air interface described by the height function $h(x)$ is calculated using the line integral given in equation [7] when $Ak << 1$.

$$L = \int_{-2\pi/k}^{2\pi/k} \sqrt{1+\left(\frac{dh(x)}{dx}\right)^2}\, dx \approx \int_{-2\pi/k}^{2\pi/k} \left[1+\frac{1}{2}\left(\frac{dh(x)}{dx}\right)^2\right] dx = \frac{4\pi}{k}\left[1+\left(\frac{Ak}{4}\right)^2\right] \qquad [7]$$

Minimising the total energy of the system $W = W_E + W_S$ with respect to A yields equation [8] where W_E is given in equation [6], $W_S = \gamma L$ is the surface free energy per unit length in the z-direction, γ is the surface tension at the liquid/air interface, and $\Delta\varepsilon$ is defined in section 3.

$$A = \frac{\varepsilon_O \varepsilon_{oil}}{\gamma} \frac{\Delta\varepsilon^2 \exp\left(-2\pi\bar{h}/p\right)}{2\left(1+\Delta\varepsilon\exp\left(-2\pi\bar{h}/p\right)\right)^2} V_O^2 \qquad [8]$$

The peak to peak amplitude A of the sinusoidal distortion at the liquid/air interface is plotted as a function of the peak voltage V_o of the sinusoidal potential applied at $y = 0$ in figures 6 and 7. The solid lines were calculated from the numerical solution of the Maxwell equation [2] and equation [7] and the dashed lines show the predictions of the analytical approximation given by equation [8], with $\gamma = 0.025$ N m^{-1} and $p = 100$ μm in both cases. In figure 6 curves are shown for the ratio $\bar{h}/p$ in the range $0.03 < \bar{h}/p < 0.5$ when $\varepsilon_{oil} = 8.0$ and in figure 7 curves are shown for the relative permittivity of the liquid ε_{oil} in the range $1.5 < \varepsilon_{oil} < 20$ when $\bar{h}/p = 0.25$. The analytical form of A versus V_o curves predicted by equation [8] follows a simple V_o^2 dependence. The numerical curves converge towards the corresponding analytical solutions as $V_o \to 0$ in figures 6 and 7. In this limit the gradients of the curves increase monotonically as either the ratio $\bar{h}/p$ is decreased or the value of relative permittivity of the liquid ε_{oil} is increased, which indicates how the wrinkle amplitude can be maximised for a given applied voltage.

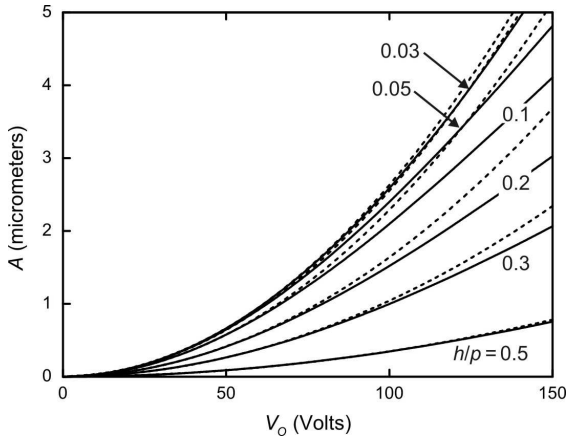

Figure 6. The peak to peak amplitude A of the sinusoidal "wrinkle" distortion as a function of the peak value V_o of the sinusoidal potential applied at $y = 0$. The solid lines were calculated from the numerical solution of the Maxwell equation [2] and the dashed lines show the predictions of the analytical approximation given by equation [8] with $\gamma = 0.025$ N m^{-1} and $p = 100$ μm. For each value of the ratio $\bar{h}/p$ the analytical prediction tends to the corresponding numerical solution in the limit $V_o \to 0$.

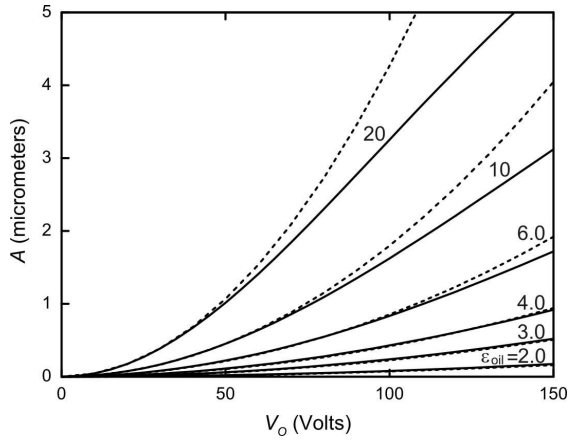

Figure 7. The peak to peak amplitude A of the sinusoidal "wrinkle" distortion as a function of the peak value V_o of the sinusoidal potential applied at $y = 0$. The solid lines were calculated from the numerical solution of the Maxwell equation [2] and the dashed lines show the predictions of the analytical approximation given by equation [8] with $\gamma = 0.025$ N m^{-1} and $p = 100$ μm. For each value of the relative permittivity of oil ε_{oil} the analytical prediction tends to the corresponding numerical solution in the limit $V_o \to 0$.

The analytical expression in equation [8] was derived using the assumption $Ak << 1$ and very close agreement between the analytical and numerical calculations for the electrostatic energy of the system (within 1% for example) is found for $Ak \approx 0.05$, as shown in figures 4 and 5. Since figures 6 and 7 were calculated with $p = 100$ μm this value corresponds to $A \approx 0.8$ μm. The analytical and numerical predictions agree closely for $\bar{h} / p = 0.5$ in figure 6 and for $\varepsilon_{oil} = 2.0$, 3.0, or 4.0 in figure 7 since the amplitude A remains below 1 μm for the range of voltage shown in the figures. As the peak voltage V_o is increased and the amplitude A rises significantly above 1 μm the value predicted by the numerical simulations falls below the V_o^2 dependence. In the high voltage limit as $V_o \to \infty$, which is not shown in figures 6 and 7, the amplitude A predicted by the numerical simulations (but not by the analytical expression) asymptotes towards the value at which W_E shows a minimum. This asymptotic value is determined by the particular combination of the parameters $\bar{h}$, p, V_O and ε_{Oil}, and not by the value of the surface tension γ.

5. Conclusions and future work

Equation [8] is valid in the limit $Ak << 1$, but provides useful insight when designing practical devices into the scaling dependences of the amplitude of the wrinkle A on the key geometrical and material parameters. For example, in a diffractive light modulation device a relatively small, fixed, wrinkle amplitude of $A = 0.7$–0.9 μm (depending on the refractive index of the liquid) at 543 nm wavelength is required to extinguish the zero order of coherent light transmitted through a transparent liquid [5].

In the current paper a sinusoidal deformation is assumed at the oil/air interface, equation [1], which is sufficient to describe the interface deformation when the potential at the lower boundary, $V(x,0) = V_O \cos(½kx)$, is also a single mode sinusoidal function of the coordinate x. We have shown that this model system is readily accessible to analytical solution. In a practical device a potential can be applied at the lower boundary of the liquid layer using a 1-dimensional array of interdigital conducting co-planar stripes where neighbouring electrodes are alternately biased [11]. In discussing particle based DEP applications the potential $V(x,0)$ has been approximated by a series expansion in this geometry [12] [13]. It has also been found that the liquid/air wrinkle deformation discussed here can show a non-sinusoidal profile in experimental devices when the film thickness becomes small compared to the pitch, $\bar{h} << p$ [14].

The current analytical approach could be extended towards describing the practical device geometry by allowing a non-sinusoidal deformation at the oil/air interface with the inclusion of the next term in a Fourier series in equation [9] and as well as using the Fourier series in equation [10] to simulate a more realistic electrode geometry.

$$h(x) = h - ½A_1 \cos(kx) - ½A_2 \cos(2kx) \qquad [9]$$

$$V(x,0) = \sum_i V_i \cos(½ikx) \qquad [10]$$

The 2-dimensional potentials $V_{oil}(x,y)$ and $V_{air}(x,y)$ should also then be expressed as Fourier series up to arbitrary order with coefficients determined by boundary conditions for which coefficients of even terms will be zero due to the symmetry of the system. To first order this model system will yield an expression for A_1 with a leading term containing V_1^2 (equation [8]) and with additional terms containing the products $V_i V_{i+2}$ where $i = 1, 3, 5 \ldots$ etc. The expression for A_2 will to first order only have terms with the products $V_i V_{i+2}$ as a result of the symmetry. A non-sinsuoidal

interface deformation will therefore only arise when the potential boundary condition $V(x,0)$ is also non-sinusoidal and the relative size of the A_2 will then be determined solely by the higher frequency components of the lower boundary potential and not the fundamental spatial frequency. The calculation of the tangential and normal components of the electric fields at the liquid/air interface in this approach would also enable a description of the time evolution of the different orders in the series describing the profile $h(x)$.

References

[1] T.B. Jones, M. Gunji, M. Washizu and M.J. Feldman, *J. Appl. Phys.* **89** (3), 1441 (2001)

[2] T.B. Jones, *J. Electrostat.* **51-52**, 290 (2001)

[3] C-C. Cheng, C. A. Chang and J. A. Yeh, *Optics Express* **14** (9), pp 4101-4106 (2006)

[4] C-C. Cheng and J.A. Yeh, *Optics Express* **15** (12), pp 7140-7145 (2007)

[5] C.V. Brown, G.G. Wells, M.I. Newton and G. McHale, *Nat. Photon.* **3** (7), pp 403-405 July (2009).

[6] C.G. Tsai and J.A. Yeh, *Optics Letters* **35** (14), pp 2484-2486 (2010)

[7] H. Pellat, *C. R. Acad. Sci. Paris* **119**, 691 (1895)

[8] "Dielectrophoresis: The behaviour of neutral matter in non-uniform electric fields.", H.A. Pohl, Cambridge Monographs on Physics: Cambridge University Press, Cambridge (1978)

[9] C.V. Brown, W. Al-Shabib, G.G. Wells, G. McHale and M.I. Newton, *Appl. Phys. Lett.* **97**, pp 242904-242906 (2010)

[10] "Numerical Recipes in C++: The Art of Scientific Computing", 2nd edition, W.H. Press, S.A. Teukolsky, W. Vetterling and B.P. Flannery, Cambridge University Press, Cambridge, (2002) ISBN 0521750334

[11] A. V. Mamishev, K. Sundara-Rajan, F. Yang, Y. Du and M. Zahn, *Proc. IEEE* **92** (5) pp 808-845 (2004)

[12] H. Morgan, A.G. Izquierdo, D. Bakewell, N.G. Green and A. Ramos, *J. Phys. D: Appl. Phys.* **34**, pp 1553–1561 (2001)

[13] M. W. den Otter, *Sens. Act. A* **96**, pp 140-144 (2002)

[14] G. G. Wells, C. L. Trabi, C. V. Brown, *Proc. SPIE*, **7716**, paper 77160G (2010)

Appendix

Expressions are given below for the coefficients of the Fourier modes a_1, a_3, b_1 and b_3 in equation [3] and c_1, and c_3 in equation [4] to first order in Ak.

$$a_1 = \frac{1}{\Delta\varepsilon \exp\left(-k\bar{h}\right)+1} V_O + \frac{\Delta\varepsilon^2 \exp\left(-k\bar{h}\right)}{4\left(\Delta\varepsilon \exp\left(-k\bar{h}\right)+1\right)^2} AkV_O$$

$$b_1 = \frac{\Delta\varepsilon \exp\left(-k\bar{h}\right)}{\Delta\varepsilon \exp\left(-k\bar{h}\right)+1} V_O - \frac{\Delta\varepsilon^2 \exp\left(-k\bar{h}\right)}{4\left(\Delta\varepsilon \exp\left(-k\bar{h}\right)+1\right)^2} AkV_O$$

$$c_1 = \frac{\left(\Delta\varepsilon+1\right)}{\Delta\varepsilon \exp\left(-k\bar{h}\right)+1} V_O - \frac{\Delta\varepsilon\left(\Delta\varepsilon+1\right)}{4\left(\Delta\varepsilon \exp\left(-k\bar{h}\right)+1\right)^2} AkV_O$$

$$a_3 = -\frac{\Delta\varepsilon \exp\left(-2k\bar{h}\right)}{4\left(\Delta\varepsilon \exp\left(-k\bar{h}\right)+1\right)\left(\Delta\varepsilon \exp\left(-3k\bar{h}\right)+1\right)} AkV_O$$

$$b_3 = -a_3$$

$$c_3 = -\frac{\Delta\varepsilon\left(\Delta\varepsilon+1\right)\exp\left(-2k\bar{h}\right)}{4\left(\Delta\varepsilon \exp\left(-k\bar{h}\right)+1\right)\left(\Delta\varepsilon \exp\left(-3k\bar{h}\right)+1\right)} AkV_O$$